Proc. of National Conf. on Emerging Trends in Nano Technology and Innovations in Design and Manufacturing, Rourkela, Feb 18-19, 2006, p 321-332.

Modelling And Development Of A Horizontal Vibratory Rod Mill For Mechanical Alloying: A First Report

P.K. RAY[1], P.K. RAY[2], V. SUNDAR RAJA[3], B.S. MURTY[1], K. CHATTOPADHYAY[3]

[1]Department of Metallurgical and Materials Engineering, IIT Madras, Chennai 600 036
[2] Department of Mechanical Engineering, National Institute of Technology, Rourkela 769 008
[3]Department of Metallurgy, Indian Institute of Science, Bangalore 560 012

Abstract: The present work deals with the development of a horizontal vibratory rod mill for mechanical alloying and synthesis of nanostructured materials. A simplistic model for optimization of milling efficiency has been developed, and the optimal operating parameters have been theoretically identified. The significance of developing such a mill lies in the possibility of high temperature mechanical alloying, which can open up new vistas for synthesis of nanoscale alloys.

Keywords: mechanical alloying, congruent melting intermetallics, rod mill, nanostructured materials.

INTRODUCTION

Increased demand for high performance materials has been the key driver for modern day materials research. It is now an established fact that materials processed under conditions far away from equilibrium possess extraordinary properties which render them more useful than their conventional counterparts. One of the most common non-equilibrium processing techniques is high-energy mechanical milling. Mechanical alloying involves alloying of the powders at elemental level. The mechanical milling technique was first used effectively for the purpose of alloying by Benjamin, in 1966 [1].

This technique has been used effectively to provide a large number of metastable materials with unique properties [2-4]. Some of the advanced materials synthesized by these routes include supersaturated solid solutions, amorphous and nanocrystalline materials, as well as metastable intermetallics. Amongst the materials in the last category, namely metastable intermetallics, transition metal silicides enjoy tremendous technological importance due to their excellent structural and electronic properties. One such material is nickel silicides. Nickel silicides have been found to exhibit excellent low-resistant ohmic contacts and also as contacts for Schottky barrier infrared detectors [5-10].

However, the high melting temperatures of these materials present considerable difficulties when processed by conventional routes. In this context, mechanical alloying has the potential to emerge as an attractive alternative for processing of silicides. The effect of temperature on phase selection during milling is still a grey area. The presence of a large number of congruent as well as non-congruent melting intermetallics, some of them very close to each other in the binary phase diagram offer excellent scope for fundamental studies as a function of milling temperature.

The central problem addressed in the present work is to a mill whose geometry would be amenable to be fitted to a furnace and thus be adapted for high temperature milling. Efforts have been made to elucidate this issue from a theoretical perspective.

PHYSICS OF MILLING

The horizontal vibratory rod mill

The horizontal vibratory rod mill has been designed keeping in view the geometry which would be compatible with a standard furnace. The standard ball mills like the SPEX, P5 or P7 all have complicated motions which prevent a suitable implementation of heating system. The inherent design of the present mill calls for the use of rods as milling media as opposed to balls.

The mill has two different motions – rotation about a horizontal axis and vibration in the vertical plane. The role of vibration is two-fold – on one hand it helps in disturbing a perfect rotary motion, ensuring that milling media do get detached from the vial wall and crash down; on the other hand they also result in rotation of the rods about its own axis. Consequently, due to this rotation, the entrapped powders get sheared as well. This presents a dual advantage of having shear as well as impact conditions.

The vibrations are generated by a cam fitted to the 'vibration motor'. The cam, in course of its motion lifts the roller directly on top of it. The roller in turn is connected to a platform on which the 'rotary motor' is mounted by means of a shaft. The two platforms are interconnected by four springs as shown in the figure below. Ultimately, it is the force resulting from the spring deformation which results in the vibrations. The mill is shown schematically in Fig.1.

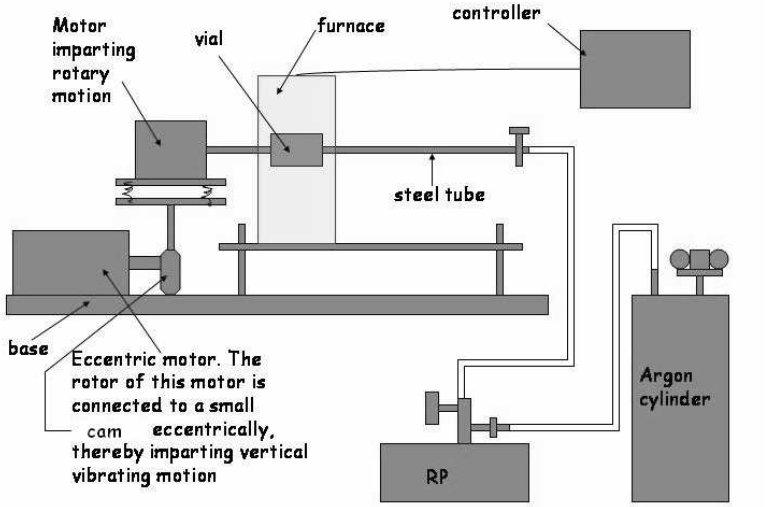

Fig 1. Block diagram of the horizontal vibratory rod mill.

Mathematical formulation of rod motion

A Cartesian reference system is chosen. The coordinate system is centered at the rotor of the motor providing vibrations.

Kinematic equations

The entire motion is considered in an *x-y* plane, on a cross section of the vial perpendicular to its axis of rotation. The reference frame is centered at the rotor of the vibration motor. The rod is assumed to move on the vial wall under no slip conditions. The equations have been developed for a two-dimensional case considering a cross section perpendicular to the central axis of the vial, as shown in fig. 2. Furthermore, it is assumed that due to the high frictional forces between the rod and the vial wall, there is no relative slipping prior to the detachment event.

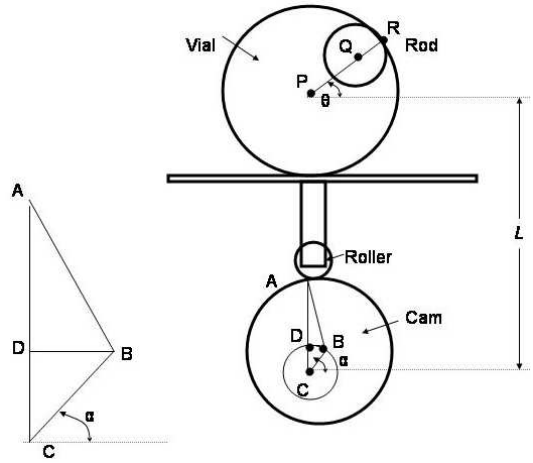

Fig 2. Defining the problem

Concentrating only on the rotation of the rod while sticking to the vial walls around the vial axis, the following equations may be written –

$$x = r_0 \cos(\omega_r t) \quad 1a$$

$$y = r_0 \sin(\omega_r t) + l - (r_d - r_d \sin \omega_v t) \quad 1b$$

where $r_0 = r_v - r_r$

Here (x,y) denotes the coordinates of the rod. r_v and r_r are the radii of the vial and the rod respectively. ω_r denotes the angular velocity with which the vial rotates and t is the time elapsed after initiation of rod motion. ω_v is the angular velocity of the cam (vibration motor) and l is the distance between the centre of the cam (vibration motor) to the centre of the vial when it is at the highest point.

The velocity components of the rod may be given as

$$v_x = \frac{dx}{dt} = -\omega_r r_0 \sin(\omega_r t) \quad 2a$$

$$v_y = \frac{dy}{dt} = \omega_r r_0 \cos(\omega_r t) + \omega_v r_d \cos(\omega_v t) \quad 2b$$

Similarly, the acceleration is given by

$$a_x = \frac{d^2 x}{dt^2} = -\omega_r^2 r_0 \cos(\omega_r t) \quad 3a$$

$$a_y = \frac{d^2 y}{dt^2} = -[\omega_v^2 r_d \sin(\omega_v t) + \omega_r^2 r_0 \sin(\omega_r t)] \quad 3b$$

The detachment event

The condition for detachment event can be found out by equating the forces acting on the rods at the instant, with the vial reaction, and consequently the frictional force, being set to zero. Forces acting on the rod at this instant are shown in the free body diagram of the rod in fig 3. If z be the spring deformation, equating the components of the forces in the radial direction, we get

$$N = m\omega_r^2 r_0 - kz\cos\left(\frac{\pi}{2} - \theta\right) - mg\cos\left(\frac{\pi}{2} - \theta\right) \quad 4$$

Also, from the fundamental equation of dynamics we get

$$\vec{\mathbf{N}} = m\vec{\mathbf{a}} \quad 5$$

The acceleration of the rod just at the moment of detachment is given by 3. This can be resolved along the radial direction and used in eqn. 5. Resolving the acceleration components along radial direction, we get

$$a_x(r) = -\omega_r^2 r_0 \cos(\omega_r t).\cos\theta \quad 6a$$

$$a_y(r) = -[\omega_v^2 r_d \sin(\omega_v t) + \omega_r^2 r_0 \sin(\omega_r t)].\sin\theta \quad 6b$$

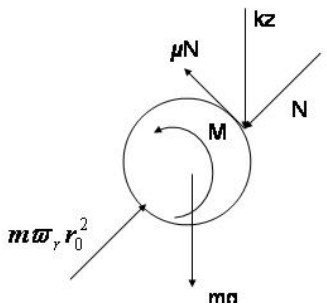

Fig 3. Free body diagram of the rod

Substituting the values of vial reaction and rod acceleration in eqn. 5, and realizing that $\theta=\omega_r t$, $\alpha=\omega_v t$, we get

$$m\omega_r^2 r_0 - kz\sin\theta - mg\sin\theta = -m\left(\omega_r^2 r_0\cos^2\theta + \omega_v^2 r_d \sin\alpha\sin\theta + \omega_r^2 r_0 \sin^2\theta\right)$$

Simplifying the above expression,

$$\sin\theta = \frac{2m\omega_r^2 r_0}{(k - m\omega_v^2) r_d \sin\alpha + mg} \qquad 7$$

The above equation defines the angle of detachment in terms of the other milling parameters. Since the value of $\sin\theta$ lies in the interval [-1,1], it is clear that detachment will not occur when the *RHS* value in the eq 7 falls outside the interval. So, considering the first case, detachment will not occur if $\sin\theta > 1$ or

$$\omega_r > \sqrt{\frac{(k - m\omega_v^2) r_d \sin\alpha + mg}{2mr_0}} \qquad 8a$$

For obtaining real values from the above expression, the numerator should be positive. Hence we arrive at the relation

$$\sin\alpha > \frac{m(\omega_v^2 r_d - g)}{k} \qquad 8b$$

This condition may be used to optimize the rotation of the individual motors along with the spring stiffness constant. Clearly, all other things being constant, the *RHS* in the above expression takes the minimum value when $\sin\alpha$ = -1 and maximum when $\sin\alpha$ = 1. This suggests that detachment event would be different for different cycles. However, it would be reasonable to assume that over a sufficiently large period of time, a sequence of cycles will be repeated, and hence one can proceed with the averaged expression as representative of the entire process. The fluctuating value of the *RHS* implies that there is a chance that for an arbitrary value of ω_r, one may have a case where detachments occur during some cycles, but not for others. In order to avoid such a situation, one should ensure that detachment occurs even for the minimum value of the *RHS* expression. This can be done by setting the condition ω_r remains less than the *RHS* expression with sinα set to -1 or α set as $(4p+3)\pi/2$, where p is a whole number. Hence the condition for having detachment in each cycle is

$$\omega_r < \sqrt{\frac{mg - (k - m\omega_v^2) r_d}{2mr_0}} \qquad 9$$

The second case arises when $\sin\theta$ < -1. Since the numerator in the *RHS* of the eqn. 7, for a negative value of $\sin\theta$, the denominator should be negative. Proceeding with a negative value of denominator and using the inequality $\sin\theta$ < -1, it is clear that this reduces to the relation 8.

Energy transfer in the mill

From the kinematic equations and the detachment criteria derived above, the collision coordinates may be described, and the energy transfer at the instant of collision calculated.

Collisions

The relatively large size of the rods, both in length as well as diameter, ensures almost complete filling of vials. Hence, unlike the popular ball-milling models, one cannot neglect the collisions between the milling media. In fact, added to this factor, the rotation of the rods about their own axis lends a large component of shear to the entire process. Based on symmetry, one may consider all the rods as equivalent (prior to detachment). Hence, considering the full packing of vial doesn't occur, and there is always some clearance, we can safely ignore the interaction between consecutive rods moving around the vial. Hence, while modelling of collisions, one has to account for the possibility of the collisions between the rods themselves, as well as the detached rod and the vial wall, while ignoring other interactions.

If the net time of flight is t_f, then one can get the collision coordinates by solving the equations of motions of all the rods. Since the only force acting on the rod once it leaves contact with the vial wall is gravity, the equations, for the detached rod would be

$$x_1 = x_d + v_x t \qquad 10a$$

$$y_1 = y_d + v_y t - \frac{1}{2} g t_f^2 \qquad 10b$$

where x_d and y_d are the detachment coordinates which may be easily found out from eqn. 1 once the value of θ and α are known. These angular values, of course, become known as soon as the other parameters, e.g. angular speed, rod mass, etc is known.

Assuming the milling to be carried out with n rods, the angular relation between the detached rod, when it is just about to get detached, and the i^{th} rod is

$$\theta_i = \theta + (i-1)\frac{2\pi}{n} \qquad 11$$

Here, the detached rod has the value i=1.

The eqn. 11 can then be used in tandem with eqn. 10. Hence the coordinates of the i^{th} rod during collision is given by

$$x_i = r_0 \cos\left[\left(\theta + (i-1)\frac{2\pi}{n}\right)t_f\right] \qquad 12a$$

$$y_i = r_0 \sin\left[\left(\theta + (i-1)\frac{2\pi}{n}\right)t_f\right] + l - \left[r_d - r_d \sin(\omega_v t_f)\right] \qquad 12b$$

It further follows that the closest distance of approach between the two rods would be equal to the sum of their radii r_{eff}. The rods being dimensionally equivalent, r_{eff} amounts to their diameter $2r_d$. This leads to the relation

$$(x_1 - x_i)^2 + (y_1 - y_i)^2 = 4r_d^2 \qquad 13$$

The equations 10, 12 and 13, when solved simultaneously will give the collision coordinates. However, the transcendental nature of these equations precludes an analytical solution, and hence an iterative (with respect to time) numerical approach is required. In such an approach, the equations 10 and 12 will be evaluated after each time step, and subjected to the following check

$$(x_1 - x_i)^2 + (y_1 - y_i)^2 \le 4r_d^2 \qquad 14$$

If this criterion is satisfied, then it is implicit that collision has occurred in the time step under consideration, and the collision coordinates can be given by the average of the coordinates of the two rods at the start and at the end of the time step under consideration. The iteration scheme is then broken. If the condition is violated, it means that collision has not occurred, and the iteration has to continue.

In the case of collision between the detached rod and the vial wall, a similar approach may be adopted, with minor modifications. Instead of considering an i^{th} rod, we need to consider the circumference of the vial to be composed of q arcs f equal length. The degree of accuracy would be higher for larger q values. The arc which is touched by the rod as it leaves contact would then be considered as the 1st arc, and the other arcs would then be numbered accordingly. Suppose, during the collision, the detached rod hits the j^{th} arc, the collision coordinates for the rod will be given by eqn. 10. The coordinates of the arc will be given by an equation similar to eqn. 12, with slight modifications. The new expression will then be given by

$$x_j = r_v \cos\left[\left(\theta + (j-1)\frac{2\pi}{q}\right)t_f\right] \qquad 15a$$

$$y_j = r_v \sin\left[\left(\theta + (j-1)\frac{2\pi}{q}\right)t_f\right] + l - \left[r_d - r_d \sin(\omega_v t_f)\right] \qquad 15b$$

The closest approach between the rod's center and the point on the arc would be attained during the collision and would equal the rod's radius. Hence, we have the condition

$$(x_1 - x_j)^2 + (y_1 - y_j)^2 = r_r^2 \qquad 16$$

In principle, the simultaneous solution of eqns. 10, 15 and 16 should describe the collisions. However, once again due to the complex nature of the equations involved, we need to resort to a time-iterative numerical approach, with the following check being performed at the end of each time step.

$$(x_1 - x_j)^2 + (y_1 - y_j)^2 \le r_r^2 \qquad 17$$

If this criterion is satisfied, then it is implicit that collision has occurred in the time step under consideration, and the collision coordinates can be given by the average of the coordinates of the two rods at the start and at the end of the time step under consideration. The iteration scheme is then broken. If the condition is violated, it means that collision has not occurred, and the iteration has to continue.

Impact frequency and energy

The average frequency of the impacts is given by

$$f = \frac{p\omega_r}{2\pi} \qquad 18$$

where p is the average number of collisions per cycle. For the sake of simplicity, assuming a reasonable high value of ω_r, p can be taken as equal to 1.

Assuming the collisions to be plastic, it can be assumed that there is a complete transfer of the kinetic energy. Due to the small diameter of the vial, the vertical movement of the rods would be less, and the contribution of the gravitational potential energy would be negligible. In such a case, the energy transferred would be given by

$$E = \frac{1}{2} m|v|^2 \qquad 19$$

Shear forces acting on the powders

Unlike ball mills, the larger contact area of the rods results in generation of shear forces in addition to the impact. In fact, it is believed that shear is the predominant mode in a rod mill. The shear forces may come into the picture in two ways. Firstly, the shearing may be manifested due to the motion of the rods against the vial walls. Secondly, they may arise due to the rubbing action between the two colliding rods. In this section we evaluate the shear forces acting on the powders due to milling.

Shearing of powders due to rod-rod contact

The force that acts is only the gravity force. Due to the spinning of the balls there will be a tangential (shear) stress acting on the powder particles entrapped between the two colliding rods. The shear stress will then be given by

$$\tau = \mu . p_r = \mu\left(\frac{W_r}{A}\right) \qquad 20$$

Where μ = coefficient of friction between rod and powder particles, p_r = pressure in the radial direction, A = contact area, W_r = component of weight of the falling rod in the direction of the line joining the rod centers (fig.4).

Since W is small, the shear stress produced thus will be small.

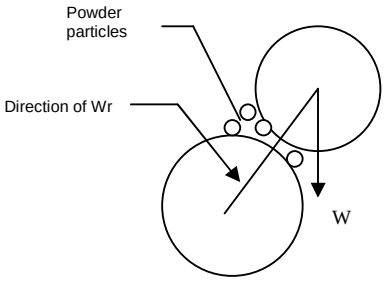

Fig 4. Shearing of powders due to rod-rod collisions

Shearing of powders due to rod-vial contact

Since the rod sticks to the vial wall due to a large centrifugal force, the contact of rod with the vial wall may be assumed to be of Hertzian type.

The maximum pressure in this case occurs at the middle length of the rod and is given by

$$p_{\max} = \frac{2N_c}{\pi . l_r b} \qquad 21$$

And the average pressure is given by

$$p_{av} = \frac{N_c}{2 . l_r b} \qquad 22$$

where N_C is the normal force between the rod and the vial wall (i.e. the centrifugal force $m\omega^2 r$, m is mass of rod) and b is the half length of Hertzian contact given by

$$b = \left[\left(\frac{1-\nu_1^2}{E_2} + \frac{1-\nu_2^2}{E_2} \right) . \frac{\pi}{4} . \frac{N_c . r}{l_r} \right]^{1/2} \quad 23$$

where ν_1, ν_2 are the Poissson's ratios of the rod and vial materials respectively, E_1, E_2 are the modulus of elasticity of the rod and vial materials respectively, and

$$\frac{1}{r} = \frac{1}{R_r} + \frac{1}{R_v} \quad 24$$

The average shear stress due to rotation of the vial during the contact period of the rod with the vial wall is

$$\tau = \mu . p_{av} \quad 25$$

where μ is the coefficient of friction between the rod-powder and vial-powder.

There will be one more component of shear due to the spinning of the rod (caused by the couple from the spring force). This is given by

$$\tau = \frac{kz \sin\left(\frac{\pi}{2} - \theta\right)}{2.l_r b} \quad 26$$

Replacing the value of z, we get the expression

$$\tau = \frac{kr_d \sin\alpha \sin\left(\frac{\pi}{2} - \theta\right)}{2.l_r b} \quad 27$$

The shear stress can then be obtained by substituting the values of α and θ at the collision points.

RESULTS AND DISCUSSIONS

The mechanics of the model can be used to develop a number of predictions. These are discussed below.

Estimation of maximum permissible rotational speed

The basic aim of the model is to predict the maximum allowable rotational speed at which the detachment event can occur, and consequently the energy transfer can be improved upon. This value critical value of ω_r can be estimated using the relation 8. The variation of ω_r with ω_v is shown in fig. 5. While it is evident that increasing ω_v has an effect on a larger permissible value of ω_r, it is not too effective. This may be attributed to the fact that the vibration is transmitted through the spring, and the spring force kz has a relatively low value due to the small value of the vibration amplitude.

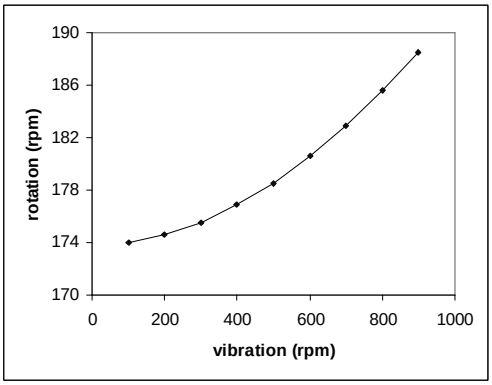

Fig. 4.8 Relation between the vibration frequency and the maximum permissible rotation speed.

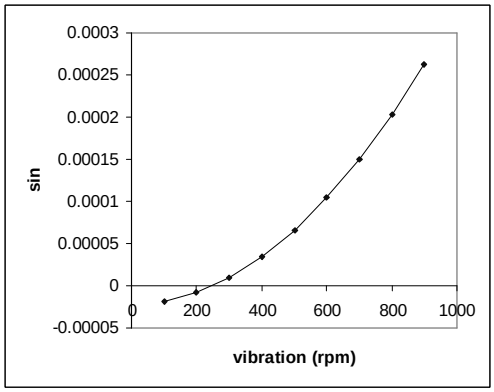

Fig. 4.9 The relation between sinα and the vibration frequency

The cam design

It is to be noted while plotting the above relation between ω_r and ω_v we have used "minimum permissible" values of $\sin\alpha$ determined in relation 9. The plot for the minimum permissible values of

$\sin\alpha$ and the vibration rpm is shown in the fig.6. It is seen that the values remain roughly close to zero. This implies that half of the values of α are suitable for having any collisions at all. By and large, the values of α which lie in the third and fourth quadrant would be unsuitable. Consequently, it is felt that the present cam design doesn't result in maximum efficiency.

This situation can be improved by a double acting cam, which would be shaped in form of an ellipse. Such a cam design would ensure that the only values that α can ever take in the mill are those in the $[-m\pi,+ m\pi]$ range. A double acting cam would ensure that effectively, α never goes outside the $[-m\pi,+ m\pi]$ interval. This ensures that the criterion for "minimum permissible" value of $\sin\alpha$ is always met, and the possible number of collisions gets doubled.

Shearing of the powders: component due to the vibrations

The major mechanism operating in rod milling is shear. Considering the geometry of the present mill, it is obvious that in addition to the standard shear components which are present in other rod mills, there is an additional shearing due to the spinning of the rods induced by vibrations. The shear stresses on the powders due to this spinning can be estimated using relation 27.

CONCLUSIONS

The phase fields evolving during ball milling differ significantly compared to the equilibrium phase fields. Size reduction of the crystallites to nano levels introduces a large number of interfaces. Hence the phases with lower interfacial energy are favored. Consequently, the non-congruent melting intermetallics get bypassed in favor of the congruent melting intermetallics. With the current mill geometry, rod milling seems to be a better option as opposed to ball milling.

Maximum milling efficiency may be realized using a proper combination of ω_r and ω_v. However, an arbitrarily large vibration frequency can't be chosen, since high frequency vibrations would prove detrimental to the mill. Based on the model, it is suggested that an operating condition of ω_r = 200 rpm and ω_v = 800 rpm would be the optimum keeping in mind the dual requirements of attaining a high energy transfer and preserving the structural integrity of the mill. The lack of alloying in the vibratory mill is ascribed to operating the mill at conditions which are reasonably far away from the optimum. In fact, as calculations in section 4.4.1 demonstrate the present operating conditions results in pinning of the rods against the vial since the rotation rpm is well above the maximum permissible frequency for even a single detachment event over an arbitrarily large number of cycles. This prevents any impact or shear due to rubbing / collisions of the rods against one another.

The milling efficiency may be further improved by modifying the cam's shape from circular (which is essentially "single action") to elliptical (which would be a "double action" case). The eccentricity of the ellipse should be chosen according to the required vibration amplitude. It has been demonstrated that the force transmitted through the spring is not too effective in initiating the detachment event by disturbing the rod's motion. Hence possible, scope exists for enhanced amplitude. The restriction to the proposed increase of the amplitude would once again be restricted by need for preserving the structural integrity in addition to the constraints imposed by the furnace size.

Shearing of the powders is seen to be strong functions of the Hertzian length. The length in turn is dependent on the radii of the rods and the vial as well as their elastic modulii. In this context, it is felt that greater vial filling (or larger rod size) would increase the shearing. However this would obviously come at the expense of impact. Also, based on the expression, it is felt that materials like tungsten carbide would be more suitable for the vial and the rods.

REFERENCES

1. J.S. Benjamin, *Metall. Trans.* 1 (1970) 2943.
2. B.S. Murty and S. Ranganathan, *Inter. Mater. Rev.* 43 (1998) 101.
3. C. Suryanrayana, *Prog. Mater. Sci.* 46 (2001) 1.
4. D.L. Zhang, *Prog. Mater. Sci.* 49 (2004) 537.
5. K.L. Pey, W.K. Choi, S. Chattopadhyay, H.B. Zhao, E.A. Fitzgerald, D.A. Antoniadis and P.S. Lee, *J. Vac. Sci. Tech.* A20 (2002) 1903.
6. H. Kanaya, Y. Cho, F. Hasegawa and E. Yamaka, *Jpn. J. Appl. Phys.* 29 (1990) L850.
7. J.R. Jimez, X. Xiao, J.C. Sturm, P.W. Pellegrini, *Appl. Phys. Lett.* 67 (1995) 506.
8. M.K. Dutta, S.K. Pabi and B.S. Murty, *J Appl Phys*., 2000, **87**, 8393-8400.
9. M.K. Dutta, S.K. Pabi and B.S. Murty, *Mater. Sci. Eng.*, 2000, **A284**, 219-225.
10. B.S. Murty, M.K. Datta and S.K. Pabi, *Sadhana*, 2003, **28**, 23-45.